Electrochemically Deposited Palladium as a Substrate for Self-Assembled Monolayers

Tesfaye Refera Soreta,† Jorg Strutwolf,*,†,§ and Ciara K. O'Sullivan*,†,‡

Nanobiotechnology and Bioanalysis Group, Department of Chemical Engineering, Universitat Rovira I Virgili, Avinguda Països Catalans, 26, 43007, Tarragona, Spain, and Institució Catalana de Recerca i Estudis Avançats, Passeig Lluís Companys 23, 08010 Barcelona, Spain

Received March 8, 2007. In Final Form: July 16, 2007

The vast majority of reports of self-assembled monolayers (SAMs) on metals focus on the use of gold. However, other metals, such as palladium, platinum, and silver offer advantages over gold as a substrate. In this work, palladium is electrochemically deposited from $PdCl_2$ solutions on glassy carbon electrodes to form a substrate for alkanethiol SAMs. The conditions for deposition are optimized with respect to the electrolyte, pH, and electrochemical parameters. The palladium surfaces have been characterized by scanning electron microscopy (SEM) and the surface roughness has been estimated by chronocoulometry. SAMs of alkane thiols have been formed on the palladium surfaces, and their ability to suppress a Faradaic process is used as an indication for palladium coverage on the glassy carbon. The morphology of the Pd deposit as characterized by SEM and the blocking behavior of the SAM formed on deposited Pd delivers a consistent picture of the Pd surface. It has been clearly demonstrated that, via selection of experimental conditions for the electrochemical deposition, the morphology of the palladium surface and its ability to support SAMs can be controlled. The work will be applied to create a mixed monolayer of metals, which can subsequently be used to create a mixed SAM of a biocomponent and an alkanethiol for biosensing applications.

1. Introduction

Designing electrode surfaces on a molecular level can be achieved by the chemical adsorption of alkanethiol molecules on a metal electrode surface.[1,2] The high grade of organization and stability of self-assembled monolayers (SAMs) and the potential of the functionalization of molecules within the monolayer enable a wide range of applications of SAM-modified electrode surfaces in sensing processes (e.g., biosensors).[3−7] Gold is the most popular substrate for thiol SAMs. Gold substrates can be handled in air without any oxide surface layer formation, and can survive harsh chemical treatment to remove organic contaminants because of the noble character of gold.[1] The other coinage metals (silver and copper) and platinum have also been used as substrates for thiol SAMs.[8−10] Palladium is not often used as a substrate for SAM formation, although the properties of SAMs of alkanethiols on palladium substrates offer advantages over SAM formation on other metals.[11−15] SAMs on palladium resist corrosion by solution-phase chemical etchants, regardless of the chain length and wettability of the SAM, in contrast to gold as a substrate, where hydrophobic, well-ordered, crystalline alkane films are required. This property makes SAMs on palladium superior to SAMs on gold or SAMs on silver systems for patterning microstructures by microcontact printing.[11,13] Palladium has also been employed as a substrate for SAMs used in biotechnology.[12] For characterization of alkanethiol SAMs on Pd, a variety of surface analytical techniques have been employed: contact angle measurements, optical ellipsometry, reflection absorption infrared spectroscopy, X-ray photoelectron spectroscopy, and surface plasmon resonance.[12,14] To our knowledge, no electrochemical method has been used for the characterization of SAMs formed on Pd. We report on the use of electrodeposited palladium on glassy carbon (GC) electrodes as a substrate to support thiol-based SAMs. The blocking behavior of the longer chain alkanethiol SAMs toward a redox reaction provides an indication of the completeness of the deposited palladium layer, since thiol SAMs form stable films on palladium but are not supported on bare GC. Consequently, redox reactions occur at the bare GC subareas, while electron-transfer reactions are more or less blocked by the SAM covering palladium deposits. The adsorption behavior of thiol SAMs has implications for the formation of micro- and nanostructures based on SAM formation

* Corresponding author. E-mail: ciara.osullivan@urv.cat (C.K.O.); jorg.strutwolf@fundacio.urv.cat (J.S.). Fax: +34 977 55 9667.

† Universitat Rovira I Virgili.

‡ Institució Catalana de Recerca i Estudis Avançats.

§ Visiting scientist at the University of Tübingen, Department of Chemistry, Institute of Organic Chemistry, Auf der Morgenstelle 18, 72076 Tübingen, Germany.

(1) Finklea, H. O. Self-assembled monolayers on electrodes. In *Encyclopedia of Analytical Chemistry*; Meyers, R. A., Ed.; Wiley: New York, 2000; Vol. 11, pp 10090−10115.

(2) Ulman, A. *Chem. Rev.* **1996**, *96* (4), 1533−1554.

(3) Wink, T.; van Zuilen, S. J.; Bult, A.; van Bennekom, W. P. *Analyst* **1997**, *122* (4), R43−R50.

(4) Satjapipat, M.; Sanedrin, R.; Zhou, F. M. *Langmuir* **2001**, *17* (24), 7637−7644.

(5) Frederix, F.; Bonroy, K.; Laureyn, W.; Reekmans, G.; Campitelli, A.; Dehaen, W.; Maes, G. *Langmuir* **2003**, *19* (10), 4351−4357.

(6) Gooding, J. J.; Mearns, F.; Yang, W.; Liu, J. *Electroanalysis* **2003**, *15* (2), 81−96.

(7) Chaki, N. K.; Vijayamohanan, K. *Biosens. Bioelectron.* **2002**, *17* (1−2), 1−12.

(8) Laibinis, P. E.; Whitesides, G. M. *J. Am. Chem. Soc.* **1992**, *114* (6), 1990−1995.

(9) Laibinis, P. E.; Whitesides, G. M.; Allara, D. L.; Tao, Y. T.; Parikh, A. N.; Nuzzo, R. G. *J. Am. Chem. Soc.* **1991**, *113* (19), 7152−7167.

(10) Laibinis, P. E.; Bain, C. D.; Whitesides, G. M. *J. Phys. Chem.* **1991**, *95* (18), 7017−7021.

(11) Carvalho, A.; Geissler, M.; Schmid, H.; Michel, B.; Delamarche, E. *Langmuir* **2002**, *18* (6), 2406−2412.

(12) Jiang, X.; Bruzewicz, D. A.; Thant, M. M.; Whitesides, G. M. *Anal. Chem.* **2004**, *76* (20), 6116−6121.

(13) Love, J. C.; Wolfe, D. B.; Chabinyc, M. L.; Paul, K. E.; Whitesides, G. M. *J. Am. Chem. Soc.* **2002**, *124* (8), 1576−1577.

(14) Love, J. C.; Wolfe, D. B.; Haasch, R.; Chabinyc, M. L.; Paul, K. E.; Whitesides, G. M.; Nuzzo, R. G. *J. Am. Chem. Soc.* **2003**, *125* (9), 2597−2609.

(15) Love, J. C.; Wolfe, D. B.; Paul, K. E.; Chabinyc, M. L.; Nuzzo, R. G.; Whitesides, G. M. *Abstr. Pap. Am. Chem. Soc.* **2002**, *224*, U431−U431.

10.1021/la7006777 CCC: $37.00
Published on Web 09/12/2007

on mixed metal surfaces,[16] which may serve as substrates to allow specific attachment of bioreceptor molecules.

Electrodeposition of Pd on GC electrodes is used to obtain Pd substrates. Although coating methods such as evaporation and sputtering chemical vapor deposition are an option, electrodeposition is often used for reasons of economy and/or convenience. Electrodeposition of palladium is especially attractive because palladium is seen as a replacement for gold as a contact metal in the electronic industry, in view of its excellent resistance to corrosion and wear, good solderability, and lower density.[17,18] However, the ability of palladium to catalyze hydrogen evolution and to absorb and dissolve hydrogen[19,20] poses a significant problem for the electrodeposition of Pd from aqueous solutions (hydrogen embrittlement). The evolution of hydrogen interferes with the reduction of Pd ions at the electrode surface, resulting in cracks of the deposited metal. The term hydrogen embrittlement is used to describe a variety of fracture phenomena related to the presence of hydrogen in a metal or alloy.[21] The degree of fractured areas in a Pd layer deposited onto a GC depends on the applied deposition potential or current.

In the first part of the paper, we will concentrate on Pd deposition to create a suitable substrate for SAMs. Palladium has been deposited from a wide variety of electrolytes, which can be broadly classified as alkaline, neutral, and acidic.[21,22] The morphology and material properties of the deposited palladium is greatly affected by the deposition conditions, such as temperature, transport mode (convection), composition, the pH of the electrolyte, the electrochemical technique, and associated parameters such as the use of applied potential or current. In the reported work, we have systematically investigated the influence of some critical experimental conditions on the deposition of palladium on GC electrode surfaces from an aqueous solution of two Pd−chloro complexes. Three different acidic electrolyte solutions are tested: nitric acid, buffer solutions of citrate, and acetate. For each electrolyte, the pH was adjusted between 1 and 4, if feasible. Deposition was performed using potentiodynamic, potentiostatic, and galvanostatic experiments. In the two latter cases, the influence of applied potential and current is investigated. The morphology of the deposited palladium is characterized by scanning electron microscopy (SEM).

The optimal parameters for palladium electrodeposition depends on the desired surface morphology. It will be shown how the variation of experimental conditions can be used for controlling the brightness, smoothness, graininess, and surface coverage of the deposited palladium layer, and in the second part of this report, it will be shown how these surface properties affect the alkanethiol SAM formation.

2. Experimental Section

2.1. Reagents. Palladium was deposited from a buffered solution of $PdCl_2$ and Na_2PdCl_4 (99.9%, Aldrich). The deposition baths employed were citrate buffer (consisting of 0.03 M citric acid, 0.0082 M HCl, 0.061 M NaCl, pH 2, Fluka), acetate buffer (acetic acid, sodium acetate, pH 4.65, Riedel-de Haen), and nitric acid (65%, Scharlau). The pH of the bath was adjusted by adding a diluted sodium hydroxide (98% Scharlau) solution or diluted nitric acid. Methyl viologen (98%, Aldrich) and potassium hexacyanoferrate-(III) (99%, Aldrich) were used as redox probes. For the formation of alkanethiol-based SAMs, *n*-decanethiol (96%, Aldrich) and *n*-butanethiol (99%, Aldrich) were used. All chemicals were provided by Sigma (Barcelona, Spain) and used as received without any other treatment. The solutions were prepared with Milli-Q water (18.2 MΩ·cm).

2.2. Electrode Preparation. GC rods (Sigradur, HTW Hochtemperatur Werkstoffe, Germany) with a length of 7 cm and a diameter of 3 mm were pressed into two layers of heat-shrinking polyolefine tubes. One end of the rod, which served as the electrode surface, was polished with 0.3 μm alumina slurry (BUEHLER). Upon polishing, the electrodes were carefully rinsed with Milli-Q water and sonicated for about 15 min. The electrodes were used immediately after the cleaning procedure.

For SAMs of alkanethiols, the palladinized electrodes were immersed into a 10 mM ethanolic solution of *n*-decanthiol or *n*-butanethiol for 12 h. Afterward, the electrodes were carefully flushed with ethanol and washed with water followed by air drying.

2.3. Instrumentation. *2.3.1. Electrochemical Measurements.* Cyclic voltammetry, potential step, and current step experiments were carried out using an Autolab model PGSTAT 12 potentiostat/galvanostat controlled with the General Purpose Electrochemical System (GPES) software (Eco Chemie B.V., The Netherlands). A conventional three-electrode setup was used with the GC electrode as the working electrode and a platinum wire (BAS model MW-1032) as a counter electrode. An Ag/AgCl electrode (BAS model MF-2078) served as a reference electrode. All potentials were reported with respect to this reference electrode. A magnetic stirrer provided the convective transport during potential step and galvanostatic experiments. Prior to any measurement, the solutions in the electrochemical cell were flushed with Argon gas for 5 min. All depositions were performed from solutions containing 1.33 g/L $PdCl_2$ or Na_2PdCl_4.

Because of the limited potential window, it was not possible to use potassium hexacyanoferrate to determine the area of the palladinized electrodes, and instead methyl viologen was used. The real electrode areas, taking into account the surface roughness, were determined by chronocoulometry. The duration of the potential step was 250 ms. The real electrode area of the bare GC electrode was estimated in 0.1 M aq KCl using 0.1 mM potassium hexacyanoferrate (diffusion coefficient 7.6×10^{-6} cm^2/s) using Anson's equation.[23] The real area of the deposited palladium surfaces was measured by chronocoulometry using methyl viologen dichloride. The diffusion coefficient of methyl viologen was measured by cyclic voltammetry using a bare GC electrode, and a value of $D = 6.4 \times 10^{-6}$ cm^2/s was found. Chronocoulmetric measurements with the palladium-modified electrodes using methyl viologen allows then the estimation of the real area from which the roughness factor was calculated.

2.3.2. SEM Imaging. SEM for the characterization of palladinized surfaces on a GC electrode was carried out using a Quanta 600, FEI Company model environmental scanning electron microscope at an acceleration voltage of 20 kV and a working distance of 10 mm in a high-vacuum mode.

3. Results and Discussion

Primarily studies of electrochemical Pd deposition were performed by cyclic voltammetry in unstirred solution for all conditions under investigation. All voltammograms showed the same basic shape, but with differences in the peak potentials for the reductive palladium deposition, depending on the electrolyte, pH, and Pd source, as will be discussed later. A typical example is given in Figure 1, where the first, second, and third scan for deposition from $PdCl_2$ in citrate buffer solution at pH 3 is shown. The peak potentials can be assigned to the following electrode reactions: Palladium is reductively deposited at 125 mV (first

(16) Oyamatsu, D.; Kanemoto, H.; Kuwabata, S.; Yoneyama, H. *J. Electroanal. Chem.* **2001**, *497* (1−2), 97−105.
(17) Micklus, S. G. *Plat. Surf. Finish.* **1995**, *82*, 67.
(18) Abys, J. A. *Plat. Surf. Finish* **1999**, *86*, 108−115.
(19) Lewis, F. A. *The Palladium-Hydrogen System*; Academic Press: New York, 1967.
(20) Green, T.; Britz, D. *J. Electroanal. Chem.* **1996**, *412* (1−2), 59−66.
(21) Abys, J. A.; Dullaghan, C. A. Electrodeposition of palladium and palladium alloys. In *Modern Electroplating*; Schlesinger, M., Paunovic, M., Eds.; John Wiley & Sons: New York, 2000; pp 483−553.
(22) Rao, C. R. K.; Trivedi, D. C. *Coord. Chem. Rev.* **2005**, *249* (5−6), 613−631.
(23) Anson, F. C. *Anal. Chem.* **1966**, *38* (1), 54−57.

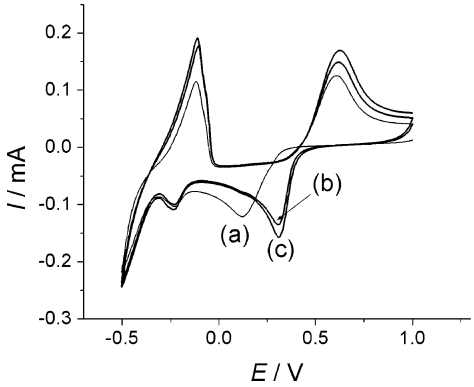

Figure 1. CVs of Pd deposition on a GC surface from a $PdCl_2$ solution in citrate buffer at pH 3: (a) first scan; (b) second scan; (c) third scan. Scan rate 50 mV/s.

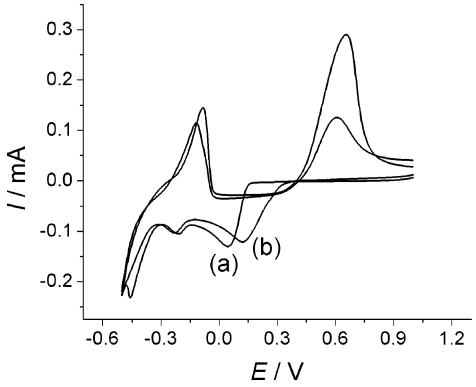

Figure 2. CV (first cyclic scan) of (a) Na_2PdCl_4 and (b) $PdCl_2$ (all conditions as in Figure 1).

scan) and 308 mV (consecutive scans). The cathodic peak at −225 mV is due to the formation of PdH_x[21] followed by a steep current increase as a result of hydrogen evolution at the negative end of the potential window. On the return scan, hydrogen is stripped off at a potential of −110 mV, and finally palladium is dissolved at 620 mV. The positive potential shift of palladium deposition process after the first scan has been observed in all electrolyte systems. It is not a concentration effect, since the deposition potential peak remains constant after the first scan. The behavior can be attributed to a nucleation effect of Pd on GC only present in the first scan. This explanation is supported by the observation of two current crossovers on the positive going scan of the first cycle, only present in the first scan.

3.1. Effect of Pd Source. The electrochemical mechanism of palladium deposition from an acid chloride system has been studied in detail.[24−29] In a chloride solution, various Pd−chloro complexes can exist, and the reduction mechanism assumes the complex dissociates sequentially to form $PdCl_2$. Only $PdCl_2$ is found to be the discharging species:[25]

$$PdCl_4^{2-} \leftrightarrow PdCl_3^{-} \leftrightarrow PdCl_2 + 2e \rightarrow Pd + 2Cl^-$$

Figure 2 shows voltammograms of the deposition from solutions prepared with $PdCl_2$ and Na_2PdCl_4. The Pd deposition peak for the more stable $PdCl_4^-$ complex is shifted by 80 mV to a more negative potential. The difference in peak potential remains constant in consecutive scans. Since interference from hydrogen co-deposition increases with more negative potential, deposition from $PdCl_2$ is thus preferable.

3.2. Effect of pH and Electrolyte. The effect of pH and electrolyte on the deposition potential of Pd was studied by cyclic voltammetry. The peak potentials for the deposition of palladium from $PdCl_2$ in three electrolyte solutions at different pH values are displayed in Table 1.

The Pd complexation ability of nitrate ions is low, even in nitric acid at very low pH values (stability constant, $\log \beta = 1.2$ at pH = 0 in aq nitric acid solution[30]), and the nitrate complexes are much less stable than those with chloride.[31] Therefore, in a pH 2 solution of $PdCl_2$ in nitric acid, Pd is present in the form of its chloro complex and we focus in the following discussion on the effect of acetate and citrate electrolytes only.

Within one sort of electrolyte solution (acetate or citrate), the potential of the deposition peak is shifted in the negative direction with increasing pH. This behavior is explained by the competition between palladium complexation by the ligand L^{n-} (acetate or citrate ion) and protonation of the ligand:

$$Pd^{2+} + nL^{m-} \Leftrightarrow PdL_n^{(mn-)+2}$$

A high proton concentration will decrease the amount of ligand ions free for the complexation of palladium ions:

$$H_mL \Leftrightarrow mH^+ + L^{m-}$$

The protonation of the ligand depends on the proton concentration and on the pK_a value of the ligand itself. The pK_{a1} value for acetic acid is 4.52, while, for citric acid, $pK_{a1} = 2.80$ and $pK_{a2} = 4.08$, indicating a higher concentration of citrate than acetate at the relevant pH values.

Since deposition from the ligand−palladium complex is energetically less favored than that from uncomplexed Pd ions, the peak potential for deposition is shifted in a negative direction with decreasing pH (within the same electrolyte).

On the other hand, hydroxide concentration plays a significant role because of the stability of hydroxo complexes. The stability constant for the reaction

$$Pd^{2+} + 2OH^- \Leftrightarrow Pd(OH)_2$$

is $\log \beta = 25.8$,[32] at pH > 3.

At higher pH values (pH > 3), stable hydroxo complexes of palladium are formed, preventing Pd deposition.

At pH > 3, the Pd deposition is limited by the formation of the stable hydroxides, which compete with the formation of Pd complexes with acetate, citrate, and nitrate, resulting in poor quality of the Pd film.

At pH 2 and 3, the complexing ability of the two ligands (acetate and citrate) listed in Table 1 can be compared. At both

(24) Bell, M. F.; Harrison, J. A. *Electroanal. Chem. Interfacial Electrochem.* **1973**, *41*, 15−25.
(25) Crosby, J. N.; Harrison, J. A.; Whitfield, T. A. *Electrochim. Acta* **1981**, *26* (11), 1647−1651.
(26) Crosby, J. N.; Harrison, J. A.; Whitfield, T. A. *Electrochim. Acta* **1982**, *27* (7), 897−902.
(27) Gimeno, Y.; Creus, A. H.; Carro, P.; Gonzalez, S.; Salvarezza, R. C.; Arvia, A. J. *J. Phys. Chem. B* **2002**, *106* (16), 4232−4244.
(28) Harrison, J. A.; Alcazar, H. B. S.; Thompson, J. *Electroanal. Chem. Interfacial Electrochem.* **1974**, *53*, 145−150.
(29) Harrison, J. A.; Hill, R. P. J.; Thompson, J. *Electroanal. Chem. Interfacial Electrochem.* **1973**, *47*, 431−440.
(30) Jorgensen, C. K.; Parthasarathy, V. *Acta Chem. Scand., Ser. A: Phys. Inorg. Chem.* **1978**, *32* (10), 957−962.
(31) Frias, E. C.; Pitsch, H.; Ly, J.; Poitrenaud, C. *Talanta* **1995**, *42* (11), 1675−1683.
(32) *Stability Constants of Metal-Ion Complexes*, 2nd ed.; Sillén, L. G., Martell, A. E., Eds.; The Chemical Society: London, 1971; p 25.

Table 1. Peak Potentials for Pd Deposition from $PdCl_2$ Using Different Electrolyte Systems and pH Values[a]

electrolyte	pH	Pd deposition peak/V
nitric acid	2	0.338
acetate	2	0.411
acetate	3	0.343
citrate	2	0.322
citrate	3	0.288
citrate	4	0.246
citrate	5	0.207

[a] The scan rate was 50 mV/s, and peak potentials are reported for the second potential cycle.

pH values, the peak potential of Pd deposition from acetate is more positive than that from citrate solution, implying that a less electrochemical driving force is necessary. This might be due to the higher pK_{a1} value of acetic acid in comparison to citric acid, resulting in lower availability of acetate ions for complexation and therefore easier electrochemical deposition from the acetate solution.

Pd was potentiodynamically deposited by cycling the potential between 0.8 and −0.5 V at a scan rate of 25 mV/s 25 times to inspect the structure and morphology of the Pd deposits by SEM. SEM images of the deposition from citrate (pH 2, 3), nitrate (pH 2), and acetate (pH 2, 3) solutions are presented in Figure 3. SEM images for deposition from citrate (pH 4 and 5) reveal a part of uncovered GC (pH 4) and the formation of isolated Pd particles (pH 5). These images are presented in the Supporting Information available for this article. The low solubility of $PdCl_2$ (hydroxide precipitation) in nitric acid at pH ≥ 3 and in acetate at pH ≥ 5 prevents deposition at these pH values. Deposition from pH 2 nitrate (Figure 3c) and pH 3 acetate (Figure 3e) did not give good coverage of the GC electrode with bare parts of the GC exposed to the solution. These media were excluded from further studies. Palladium deposition from pH 2 and 3 citrate buffer and pH 2 acetate buffer resulted in well-covered surfaces, with the pH 3 citrate system delivering the most uniform coverage, as was found by visual examination of the SEM images taken at five different locations of the surface. Therefore, for subsequent studies, the choice was palladium deposition from citrate buffer at pH 3.

3.3. Potentiostatic and Galvanostatic Deposition. Palladium was deposited by applying constant potentials between 300 and −300 mV for 60 s in stirred citrate (pH 3) solutions. As expected, the deposition at positive potentials of 300, 200, and 100 mV, which are near the deposition peak potentials of palladium (see Figure 1), resulted in isolated palladium particles on the GC surface, as shown in Figure 4A. For more negative potentials, the amount of palladium deposited on the electrode increases, improving the surface coverage. At a step potential of −100 mV, the electrode surface is shiny silver. The mirror-like appearance indicates the high reflective power of a smooth palladium layer. In contrast, at more negative potentials, −200 mV and −300 mV, the electrode appears dark and non-shiny. The SEM images reveal a complete coverage of the electrodes but with smaller crystallites in the case of deposition at −100 mV (Figure 4B). A photograph of electrodes modified with a shiny silver and black Pd layer are presented in the Supporting Information.

The finer grain size is due to a slower growth of Pd particles at less negative potentials. The size of the crystallites increases with more negative deposition potentials (see Figure 4C). However, the effect of palladium-catalyzed hydrogen evolution and adsorption has a major effect on the structure of the deposited metal layer. The hydrogen evolution process interferes with palladium deposition and becomes more prominent with decreasing potential. Increased hydrogen evolution and adsorption might inhibit the leveling observed for a deposition potential of −100 mV (leading to a bright surface), and will produce a dark porous palladium coating instead.

The galvanostatic deposition of palladium was performed at current densities of −1.4, −2.8, −4.3, −5.7, and −7.1 mA/cm^2 (equivalent to currents of 100, 200, 300, 400, and 500 μA, respectively, on a 0.071 cm^2 electrode) for 100 s. The visible appearance of the electrode was bright and shiny for the less negative current densities, but became dark and non-reflecting for current densities of −5.7 and −7.1 mA/cm^2. Assuming 100% current efficiency, an even deposition of a compact Pd layer across the electrode surface would result in a deposition thickness between 65 and 327 nm for current densities between −1.4 and −7.1 mA/cm^2. Despite the strong decrease in the current efficiency, mainly due to hydrogen evolution, a complete coverage of the electrode with Pd (the lattice constant of pure palladium is 0.33889 nm) would have been attainable. SEM images using a 30 000× magnification (Figure 5A) reveal a relatively smooth surface for a deposition current density of −1.4 mA/cm^2 (100 s). The image shows an area uncovered by Pd. Such areas are observed in many regions across the electrode and are a result of incomplete coverage and might be introduced by hydrogen evolution, a side reaction already present at low overpotential, or, alternatively, by inhomogeneities of the GC substrate. At more negative current densities (−5.7 and −7.1 mA/cm^2) a change in the morphology is observed (Figure 5B). The Pd layer is rougher and porous, in contrast to the more compact layer deposited at −1.4 mA/cm^2. The change in morphology is due to the increasing influence of hydrogen evolution and co-deposition. However, because of the increased volume of the black Pd deposit, a better coverage of the GC electrode is achieved. This observation is analogous to the behavior for potentiostatic deposition at low and high applied potentials.

Surface roughness can be defined as the difference between the real or microscopic electrode area A_m and the geometrical or projected area A_g,[33] with the roughness factor being $\rho = A_m/A_g$. The microscopic areas of bare GC surfaces and of electrodes modified with palladium deposits were estimated by chronocoulometry in the short time range. The roughness factor measured for individual bare GC electrodes varied between $\rho = 4.4$ and 6.6. The general trend is an increase in the roughness factor ρ of the palladinized electrode with increasing absolute reduction current density, that is, an increase in roughness, as confirmed by the SEM images presented in Figure 5. For a smooth shiny Pd layer deposited at −1.4 mA/cm^2 for 100 s, ρ was estimated by chronocoulometry to be 3.38 ± 0.04, while, for the black Pd layer (−7.1 mA/cm^2), a roughness factor of 56.77 ± 0.16 was estimated. As will be shown, the surface properties of the deposited palladium has an important influence on the integrity of alkanethiol-based SAMs formed on top of the metal.

3.4. SAM Formation on Palladium. The formation and stability of alkanethiol-based SAMs on palladium has been studied by nonelectrochemical methods.[13,14] In this work, the influence of a dodecanethiol SAM formed on palladium on the redox reaction of a species in bulk solution is investigated. The ability to suppress the redox reaction of, for example, potassium hexacyanoferrate, is a measure of the integrity of the SAM. One problem encountered with the electrochemical characterization of the SAM on palladium is the accessible potential window that is limited by hydrogen evolution reaction on the cathodic side

(33) Bard, A. J.; Faulkner, L. R. *Electrochemical Methods: Fundamentals and Applications*, 2nd ed.; John Wiely & Sons: New York, 2001.

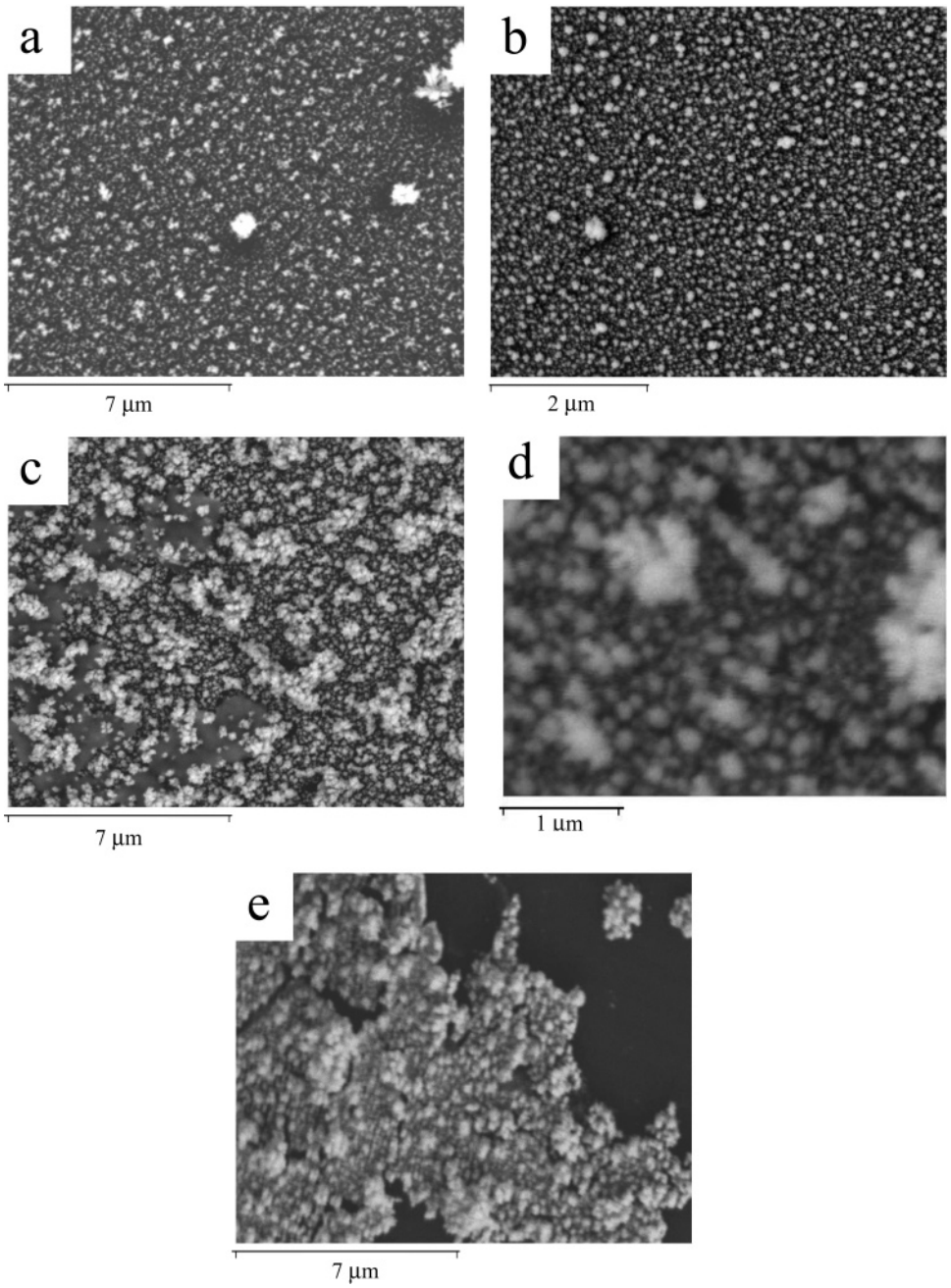

Figure 3. SEM images of palladium deposits on GC electrode by cyclic voltammetry: (a) pH 2 citrate; (b) pH 3 citrate (20 000×); (c) pH 2 HNO_3; (d) pH 2 acetate (50 000×); (e) pH 3 acetate. Magnification is 10 000× except where indicated in parentheses.

and by palladium dissolution on the anodic range. Precisely for this reason, methyl viologen was used as the redox probe instead of the more conventionally used potassium hexacyanoferrate. The electrochemistry of viologen compounds have been extensively studied by electrochemical techniques.[34] Cyclic voltammograms (CVs) showing the redox reaction of methyl viologen at GC electrodes are presented in the Supporting Information. The CV of methyl viologen (MV^{2+}) at GC electrodes exhibits two separated redox waves, which are attributed to the $MV^{2+}/MV^{+\bullet}$ ($E_{1/2} = -0.66$ V) and $MV^{+\bullet}/MV^0$ ($E_{1/2} = -1.02$ V vs Ag/AgCl) couples, respectively. The second redox wave at more negative potential is markedly affected by deposition of the neutral methyl viologen product, MV^0, unlike the first stage, $MV^{2+}/MV^{+\bullet}$, which shows the typical behavior of a reversible electron transfer without any evidence of adsorption, in agreement with other reports.[35,36] Since the first redox stage fell into the accessible potential window of the palladinized electrodes (−0.825 to −0.5V), the $MV^{2+}/MV^{+\bullet}$ redox couple was chosen for probing the integrity of SAMs formed on Pd. It was shown before that SAMs formed on gold electrodes can effectively block the $MV^{2+}/MV^{+\bullet}$ reaction.[37]

Two sets of palladinized electrodes were used for SAMs of *n*-decanethiol. The first set consists of electrodes with a mirror-like palladium surface, produced under galvanostatic (current density −1.4 mA/cm^2 for 100 s) and potentiostatic (applied potential −100mV for 60 s) conditions. The palladium surface of the second set of electrodes had a black and non-reflecting appearance, again produced by constant potential (−300 mV,

(34) Bird, C. L.; Kuhn, A. T. *Chem. Soc. Rev.* **1981**, *10* (1), 49−82.

(35) Engelman, E. E.; Evans, D. H. *Langmuir* **1992**, *8* (6), 1637−1644.
(36) Kaifer, A. E.; Bard, A. J. *J. Phys. Chem.* **1985**, *89* (22), 4876−4880.
(37) Henderson, J. I.; Feng, S.; Ferrence, G. M.; Bein, T.; Kubiak, C. P. *Inorg. Chim. Acta* **1996**, *242* (1−2), 115−124.

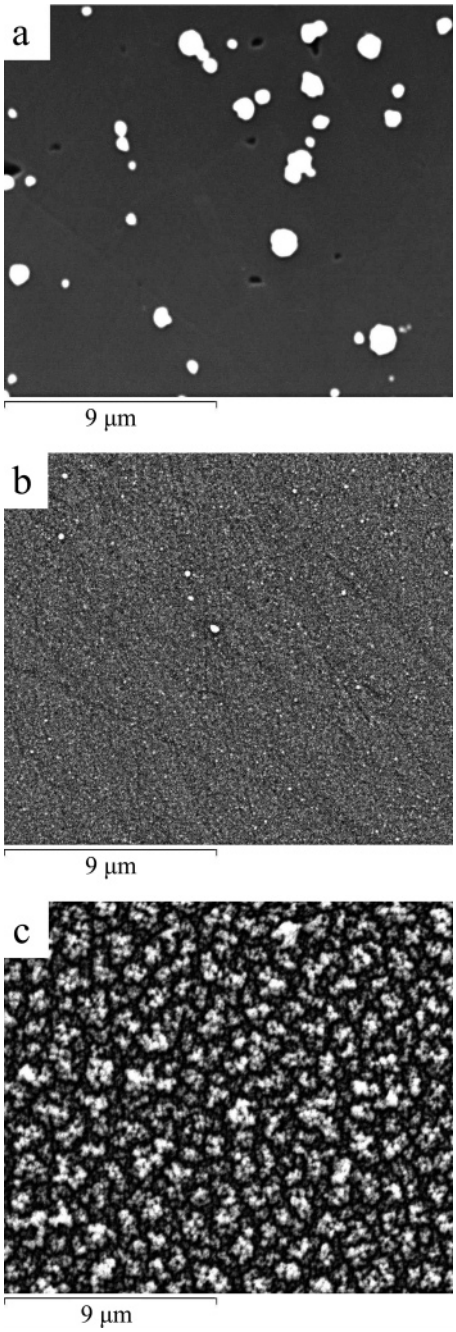

Figure 4. SEM images of palladium deposits on GC for deposition potentials (a) +0.3 V, (b) −0.1 V, and (c) −0.3 V. Magnification 8000×.

60 s) and current (−7.1 mA/cm^2, 100 s) conditions. In all cases, deposition was from a pH 3 citrate solution containing $PdCl_2$.

Examples of CVs for both kinds of electrodes using methyl viologen as a redox probe are presented in Figure 6. The CVs labeled "a" in Figure 6(i)−(iv) are recorded using the palladinized electrodes without SAM, while the CVs labeled "b" were measured with decanethiol SAM-modified Pd surfaces. Optical micrographs of the Pd surfaces are presented as insets in Figure 6(i)−(iv), showing the reflection of a 633 nm laser beam at the electrode surface. The micrographs are taken over an area of 500 × 500 μm^2. Only minor blocking of the methyl viologen redox reaction, manifested in a slight decrease of the peak currents, is observed for the SAMs on shiny palladium surfaces, both generated potentiostatically and galvanostatically. For Figure 6(i), a Pd surface produced at a deposition potential of −100 mV for 60 s was used. The highly reflective surface is characterized

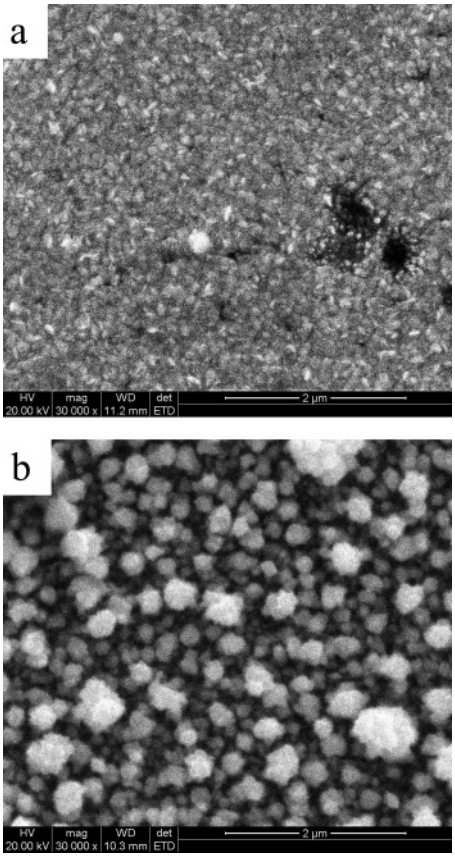

Figure 5. SEM images (magnification 30 000×) of galvanostatically deposited Pd: (a) −1.4 mA/cm^2; (b) −7.1 mA/cm^2. Deposition time 100 s.

by the bright optical micrograph, as shown in the inset of Figure 6(i). Likewise, the galvanostatically deposited Pd film (−1.4 mA/cm^2 for 100 s) shows a similar behavior (Figure 6(iii)). In contrast, monolayers assembled on the black palladium surfaces form a substantial barrier against the redox reaction, as can be seen in Figure 6(ii),(iv). The non-reflecting appearance of the Pd surface is indicated by the black micrographs. Microcracks and microholes in the shiny palladium layer, as shown in the SEM images in Figures 4B and 5A, could be the reason for the lack of blocking, since thiol-based monolayers are not assembled on GC. The redox process of methyl viologen could therefore take place at the microholes, while the *n*-decanethiol monolayer on palladium prevents redox reactions from taking place at the metal surface. This is the situation of a partially blocked electrode. However, from the size and distribution of the microholes, as shown in the SEM images, one would expect a more pronounced change in the shape of the CVs. Therefore we assume that SAM formation on the palladium of the shiny electrodes is highly incomplete, in opposition to the SAM formation on the black, non-reflecting palladium. The different behavior might be attributed to the difference in surface roughness. It is known that the quality of an alkanethiol SAM on gold improves with increasing roughness of the gold surface and the presence of crystal grain boundaries.[38,39] However, a contribution of microcracks in the thin Pd layer, as shown in Figure 5A, to the lack of blocking cannot be ruled out. The increase in roughness and thickness might be the reason that the SAM formation on the non-reflecting palladium leads to a dense blocking layer. To

(38) Creager, S. E.; Hockett, L. A.; Rowe, G. K. *Langmuir* **1992**, *8* (3), 854−861.

(39) Guo, L. H.; Facci, J. S.; McLendon, G.; Mosher, R. *Langmuir* **1994**, *10* (12), 4588−4593.

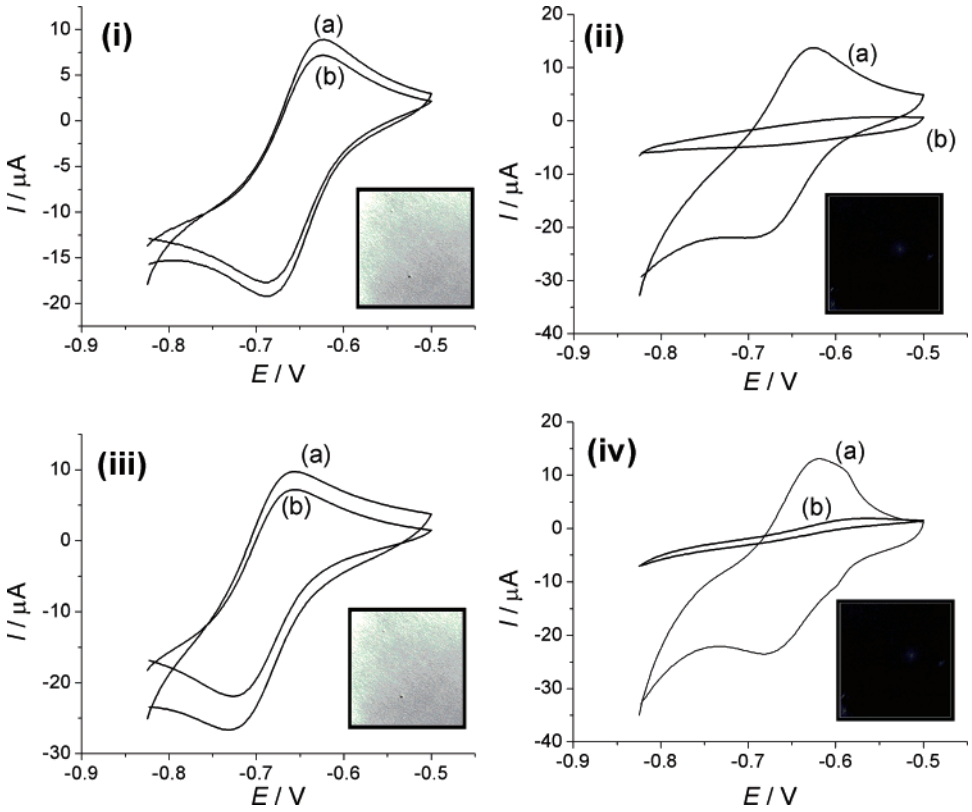

Figure 6. CVs of methyl viologen (3 mM) in 0.1 M aq KCl solution (a) before and (b) after decanethiol SAM formation. Palladium was deposited (i) potentiostatically, applied potential −100 mV (60 s); (ii) potentiostatically, applied potential −300 mV (60 s); (iii) galvanostatically, applied current density −1.4 mA/cm^2 (100 s); and (iv) galvanostatically, applied current density −7.1 mA/cm^2 (100 s). The insets are optical micrographs showing the reflection of a 633 nm laser beam scanned over an area of 500 × 500 μm^2.

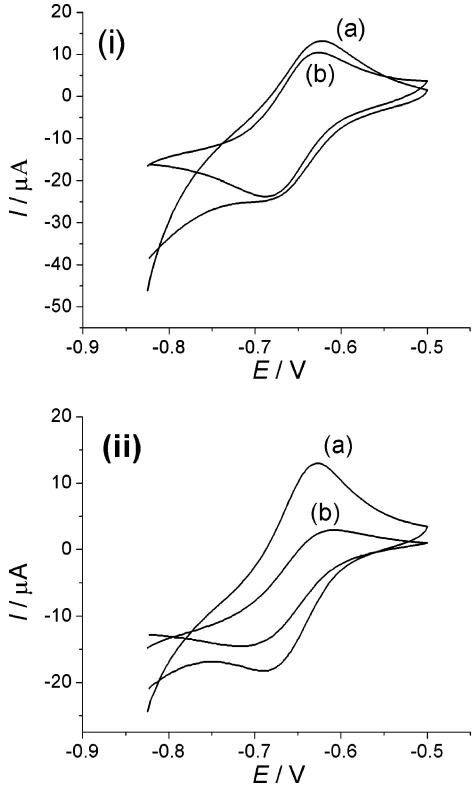

Figure 7. CVs of methyl viologen (3 mM) in 0.1 M aq KCl solution (a) before and (b) after *n*-butanethiol SAM formation. Palladium was deposited at (i) −100 mV and (ii) −300 mV for 60 s.

compare the formation of a SAM with a short- rather than long-chain alkanethiol, butanethiol was used instead of decanethiol, with the same trend being observed as shown in Figure 6. For the voltammograms shown in Figure 7(i),(ii), the Pd substrates were produced with the same conditions as in Figure 6(i),(ii), but decanethiol was replaced by butanethiol. Again, only very minor blocking is observed for the smooth Pd surface, indicated by a 5% decrease in the anodic current peak. Partial blocking can be seen for the rougher surface (Figure 7(ii)), resulting in a 57% decrease in the anodic current peak. As expected, the blocking behavior of butanethiol is not as good as that of decanethiol, since the blocking ability increases with increasing chain length.[1]

4. Conclusion

Selection of experimental conditions for the electrochemical deposition of palladium on GC allows control of the morphology of the palladium surface. This is achieved by the choice of the media (pH and type of electrolyte) from which palladium is deposited. Furthermore, the current density in the case of galvanostatic deposition and the applied potential in the case of potentiostatic deposition contribute to the microscopic structure of the Pd surface. A systematic investigation of theses factors has been performed, using SEM and electrochemical methods. The best surface coverage and the highest roughness was achieved using acetate buffer at pH 2 or citrate buffer at pH 3 and a deposition potential of −0.3 V for 60 s or a current density of −5.7 and −7.1 mA/cm^2 for 100 s. Under these conditions, decanethiol and butanethiol SAMs on the electrodeposited palladium substrate shows substantial blocking with methyl viologen redox reaction and suppresses the hydrogen evolution reaction, indicating the suitability of the substrate to support SAMs. Current efforts are focusing on the use of electrodeposition to create a mixed monolayer of metals, which can subsequently

be used to create a mixed SAM of biocomponent and alkanethiol for biosensing applications.

Acknowledgment. This paper partly describes work undertaken in the context of EC IST project Integrated Microsystem for the Magnetic Isolation and Analysis of Single Circulating Tumour Cells for Oncology Diagnostics and Therapy Follow-Up (MASCOT) FP6-2005-IST-027652. The IST programme is partially funded by the European Commission. Financial support by the SAFE Network of Excellence (LSHB-CT-2004-503243) is also acknowledged.

Supporting Information Available: Pd deposition from citrate solution at pH 4 and 5, electrochemistry of methyl viologen, and a photograph of palladinized GC electrodes. This material is available free of charge via the Internet at http://pubs.acs.org.

LA7006777